



OPEN ACCESS

EDITED BY

Peter Hosick,
Montclair State University, United States

REVIEWED BY

Bruce Rogers,
University of Central Florida, United States
Sanghyeon Ji,
German Sport University Cologne, Germany

*CORRESPONDENCE

Drake A. Eserhaut,
✉ drake.eserhaut@ku.edu

RECEIVED 02 December 2024

ACCEPTED 17 January 2025

PUBLISHED 17 February 2025

CITATION

Eserhaut DA, DeLeo JM, Provost JA,
Ackerman KE and Fry AC (2025) Monitoring
skeletal muscle oxygen saturation kinetics
during graded exercise testing in NCAA division
I female rowers.

Front. Physiol. 16:1538465.

doi: 10.3389/fphys.2025.1538465

COPYRIGHT

© 2025 Eserhaut, DeLeo, Provost, Ackerman
and Fry. This is an open-access article
distributed under the terms of the [Creative
Commons Attribution License \(CC BY\)](#). The use,
distribution or reproduction in other forums is
permitted, provided the original author(s) and
the copyright owner(s) are credited and that the
original publication in this journal is cited, in
accordance with accepted academic practice.
No use, distribution or reproduction is
permitted which does not comply with these
terms.

Monitoring skeletal muscle oxygen saturation kinetics during graded exercise testing in NCAA division I female rowers

Drake A. Eserhaut ^{1*}, Joseph M. DeLeo ^{1,2},
Jessica A. Provost ¹, Kathryn E. Ackerman ² and
Andrew C. Fry ¹

¹Jayhawk Athletic Performance Laboratory – Wu Tsai Human Performance Alliance, University of Kansas, Lawrence, KS, United States, ²Female Athlete Program – Wu Tsai Human Performance Alliance, Boston Children's Hospital, Boston, MA, United States

Purpose: The purpose of this study was to analyze changes in skeletal muscle oxygen saturation (SmO_2) kinetics during exercise in female rowers both acutely and longitudinally in relation to blood lactate (BLa). We also aimed to determine the agreement and statistical equivalence between physiological thresholds derived from SmO_2 and BLa kinetics.

Methods: Twenty-three female NCAA Division I rowers were tested throughout the 2023–2024 academic year. Of these, 11 athletes completed at least two near-infrared spectroscopy (NIRS)-equipped GXTs, with physiological data analyzed for longitudinal changes. A 7x4-min discontinuous GXT protocol was performed by all athletes. First and second SmO_2 breakpoints ($\text{SmO}_2\text{BP1}$ and $\text{SmO}_2\text{BP2}$) were estimated via piecewise linear regression modeling, and BLa thresholds (LT_1 and LT_2) were calculated using ADAPT software. Paired-samples t-tests assessed differences, and equivalence was tested using two one-sided tests (TOST). Agreement was determined using Bland-Altman analysis yielding mean differences (MD) and 95% limits of agreement (LoA). Intraclass correlation coefficients ($\text{ICC}_{2,1}$) were also calculated.

Results: No difference was found between $\text{SmO}_2\text{BP2}$ and LT_2 (MD = -5.76W [95% LoA = -38.52 to 22.25W], $p = 0.134$), moderate-to-good levels of agreement ($\text{ICC}_{2,1} = 0.67$ [95% CI: 0.36 – 0.85], $p < 0.001$), and no statistical equivalence ($p = 0.117$). This was not the case for $\text{SmO}_2\text{BP1}$ and LT_1 , with NIRS significantly underestimating LT_1 (MD = -8.14W [95% LoA = -38.90 to 27.37W], $p = 0.026$), poor-to-moderate agreement ($\text{ICC}_{2,1} = 0.24$ [95% CI: -0.13 – 0.58], $p = 0.10$), and no statistical equivalence ($p = 0.487$). Additionally, SmO_2 recovery kinetics (SmO_2resat) during 1-min rest intervals increased in response to graded increases in exercise intensity ($p < 0.001$, $\eta^2_p = 0.71$), with higher intensities appearing to blunt this effect (step 6 – step 7: MD = $-0.16\% \cdot \text{s}^{-1}$, $p = 0.69$). No statistically significant changes were observed in LT 's or SmO_2BP 's throughout the 2023–2024 season.

Conclusion: In female collegiate rowers, NIRS may be a tool that compliments BLa testing when determining the second lactate threshold (i.e., LT_2). However, significant inter-individual variability exists between $\text{SmO}_2\text{BP2}$ and LT_2 paired with a lack of statistical equivalence suggest the two are not interchangeable.

While not a standalone replacement, if used in combination with traditional BLA testing methods NIRS may be a complimentary tool that helps inform individual athlete training zone prescription.

KEYWORDS

near-infrared spectroscopy, blood lactate, physiological thresholds, longitudinal monitoring, performance testing

Introduction

The rowing stroke is a cyclic movement that can be separated into two distinct phases: the drive (propulsive) phase and the recovery phase. During the recovery phase, athletes extend their arms, rockover from their hips, then begin to fully flex the knees and hips as they glide forward on the seat with the heels slightly rising as they arrive at the catch position. During the drive phase, rowers generate propulsive force by sequentially using the legs, trunk, and arms to overcome the drag from the water and rowing shell (Nugent et al., 2020) or the resistance from the rowing ergometer. Once the rower completes the stroke, their legs are fully extended, trunk angle is typically at 20–25°, and the handle is at the furthest point towards the bow (Kleshnev, 2016). Elite rowers' power production during the rowing stroke has been reported as deriving 43% from the legs, 36% from the trunk, and 21% from the arms (Kleshnev, 2016). Yet, in order to better optimize training for the standard 2,000-m Olympic race distance (2KOrd), we should also consider specific muscle and energy system contributions to the standard 2,000-m rowing ergometer performance (2KErg).

Several studies have investigated on-water (Fleming et al., 2014) and ergometer (Janshen et al., 2009; Turpin et al., 2011; Pollock et al., 2012; Wilson et al., 1988) rowing to quantify EMG activity of various muscle groups in the legs, trunk, and arms to determine their contribution to the drive phase of the rowing stroke. Collectively across these various studies, the surface EMG studies of the lower extremities show that the drive phase is dominated by the following muscles: vastus lateralis (VL), vastus medialis (VM), gluteus maximus (GM), rectus femoris (RF), biceps femoris (BF), tibialis anterior (TibA), and gastrocnemius (Gastroc) (Fleming et al., 2014; Janshen et al., 2009; Turpin et al., 2011; Pollock et al., 2012; Wilson et al., 1988; Soper and Hume, 2004). The VL, GM, BF, and Gastroc reach peak muscle EMG activity just prior to and during peak force at the handle (Wilson et al., 1988), which is at 50% of the drive phase (Janshen et al., 2009; Wilson et al., 1988). It has been suggested that the VL contributes more to the drive phase during ergometer rowing while the VM is recruited more heavily during on-water rowing (Fleming et al., 2014). Furthermore, there is evidence of significant asymmetrical lower extremity muscle activity in sweep rowers (Janshen et al., 2009). Janshen et al. found that the VL and RF EMG activity of the inside leg of sweep rowers were 25% and 32% higher, respectively, than the outside leg (Janshen et al., 2009). Van der Zwaard et al. studied 18 elite Dutch rowers to determine the relationship of various skeletal muscle physiology characteristics and 2KErg performance (van der Zwaard et al., 2018). Van der Zwaard and colleagues evaluated the muscle volume, cross-sectional area, fascicle length, and pennation angle of the medial VL. They found that the medial VL volume explained 86% of the variance of 2KErg. Furthermore, the medial VL volume had the strongest

relationship ($r = 0.92$, $p = < 0.01$) to 2KErg when compared to muscle cross-sectional area ($r = 0.83$, $p = < 0.01$), fascicle length ($r = 0.66$, $p = < 0.05$) and pennation angle ($r = -0.06$, $p = > 0.05$) (van der Zwaard et al., 2018). Taken together, these studies emphasize that the VL is one of the primary muscles for creating power during the drive phase of the rowing stroke. Therefore, this indicates that the VL is a critical muscle to monitor and continually evaluate in the training and testing of rowers to optimize performance.

Rowers create the power to propel the boat across the 2KOrd with energy system contributions attributed 70%–77% to aerobic metabolism and 23%–30% to anaerobic metabolism (Martin and Tomescu, 2017; Hagerman, 1984). The distribution of exercise metabolism, across the 2KOrd, emphasizes the need for rowers to develop the physical attributes of endurance and maximal strength to achieve peak performance. Historically, two of the most popular methods to assess rowers' exercise metabolism and determine training zone prescription during graded exercise tests (GXT) are blood lactate (BLA) (Kindermann et al., 1979; Mader, 1976; Faude et al., 2009) and gas exchange (Bhambhani and Singh, 1985; Wasserman and McIlroy, 1964; Wasserman et al., 1973). While these methods are considered the commonly used for physiological testing and training zone prescription, they can be difficult to implement due to three primary constraints: 1) limited access to laboratory equipment; 2) lack of staff with the knowledge and expertise necessary to conduct and analyze results of the physiological testing; and 3) cost—both time and financial.

Recently, near infrared spectroscopy (NIRS) has been investigated as a non-invasive technology to potentially identify the two breakpoints associated with the first and second BLA thresholds (LT₁ and LT₂) (Batterson et al., 2023; Iannetta et al., 2017; Possamai et al., 2024; Snyder and Parmenter, 2009; Turnes et al., 2019). The use of NIRS technology directly addresses two of three primary constraints to BLA testing: a relatively low-cost tool that can be applied directly on-water in the rowing shell or on-land on the rowing ergometer, therefore bypassing the need for laboratory access. The identification of the two NIRS breakpoints is accomplished by placing a NIRS device on the primary muscle(s) that would be used during the exercise activity; in this case the VL of rowers. Once the NIRS device is positioned, the infrared light (700–900 nm) can penetrate several millimeters of tissue reaching hemoglobin, myoglobin, and cytochrome oxidase chromophores within the skeletal muscle tissue of interest. Hemoglobin and myoglobin's ability to absorb and scatter light is dependent upon whether it is bound to oxygen (O₂) or not (Barstow, 2019). Therefore, when the infrared light reaches one of these chromophores, the light signal is then sent back to the NIRS device, providing real-time data on local muscle oxygen supply and demand during exercise.

The identification and improvement of power at LT₁ and LT₂ has important performance implications for endurance sport

(Mader, 1976; Ingham et al., 2002; Mader et al., 1978). The power at 4 mmol L⁻¹, a fixed blood lactate concentration (FBLC), is often used as LT₂ has been found to be a key determinant of 2KErg performance (Ingham et al., 2002; Homer, 2014). Mark Homer, former British Rowing physiologist, found that the power at a FBLC of 4 mmol L⁻¹ was the only significant determinant of 2KErg for males and females at the U23 and Senior competition levels (Homer, 2014). Therefore, the monitoring and evaluation of power at LT₁ and LT₂ should be considered an integral part of a rowing training program. Several studies have investigated the capability of NIRS to identify LT₁ and LT₂ with evidence to support (Batterson et al., 2023; Iannetta et al., 2017; Snyder and Parmenter, 2009) and contradict its efficacy (Lanigan, 2022; Passamai et al., 2024; Turnes et al., 2019). Turnes et al. investigated the relationship between a single breakpoint in deoxygenated hemoglobin (HHb|BP), using the PortaMon NIRS device, and the anaerobic threshold (AnT) during an incremental test and its relationship to 2KErg. For clarity, HHb is different than other NIRS terms such as tissue saturation index (TSI) and skeletal muscle oxygen saturation (SmO₂), as the two later variables represent hemoglobin that is *actively bound to oxygen*, whereas HHb reflects the total volume of hemoglobin *unbound to oxygen*. Further, Turnes and colleagues defined the AnT as a FBLC of 3.5 mmol L⁻¹ determined by linear interpolation, and HHb|BP was determined via a piecewise linear regression, with the breakpoint corresponding to the estimated intercept of the two linear regression lines (Turnes et al., 2019). After estimation, HHb|BP was visually identified by two independent investigators as the inflection point between the two linear regression lines, followed by a notable plateau in HHb. They found a significant correlation between (HHb|BP) and AnT ($r = 0.63$, $p = 0.02$), with no difference between mean power at (HHb|BP) and AnT (236 vs 234 W, respectively). However, there was high typical error of estimate (10.7%) and wide 95% limits of agreement (-54.1 to 50.6 W); such high variability should caution coaches and sport scientists about using this technology with rowers (Turnes et al., 2019).

In a separate study, Possamai et al. sought to investigate the (HHb|BP) along with TSI breakpoints (TSI-BP) in four scenarios during discontinuous (3-min stages, HHb|BP₃, TSI-BP₃), continuous (1-min stages, HHb|BP₁, TSI-BP₁), and constant workload tests to determine maximal lactate steady state (MLSS) and rowing distances of 500, 1,000, 2,000, and 6,000-m to determine critical power (CP). Possamai et al. used the same methodology as Turnes et al. to determine HHb|BP and TSI-BP's (Possamai et al., 2024; Turnes et al., 2019). Power outputs at HHb|BP and AnT were no different between graded exercise test (GXT) types, however, wide 95% limits of agreement were reported suggesting high variance between NIRS and BLA based methods of AnT determination (Possamai et al., 2024). Overall, there was poor agreement and wide variability between MLSS/CP and NIRS-derived thresholds (Possamai et al., 2024).

Overall, the direction and rate of change of SmO₂ during dynamic exercise tasks provide information on the balance between skeletal muscle O₂ delivery ($m\dot{Q}O_2$) and local O₂ consumption ($m\dot{V}O_2$) (Barstow, 2019; Kirby et al., 2021). This dynamic balance has been evaluated via comparing SmO₂ from the work-steps of GXTs (SmO₂rate) to BLA concentrations, with reports that changes in SmO₂rate across a GXT may be highly

related to concomitant changes in BLA (Batterson et al., 2023; Batterson et al., 2024). More recently, additional attention has been provided to the rates of SmO₂ resaturation (SmO₂resat) during dynamic exercise tasks, as during post-exercise recovery periods skeletal muscle's demand for $m\dot{V}O_2$ is reduced. While the supply of O₂ ($m\dot{Q}O_2$) also declines during rest periods, it does so at a slower rate permitting SmO₂ to change towards a positive directionality and rise (i.e., resaturate) now that supply of O₂ exceeds local tissue consumption (Van Beekvelt et al., 2001; Behnke et al., 2009; Arnold et al., 2024). This balance of $m\dot{Q}O_2$ and $m\dot{V}O_2$ biasing greater O₂ delivery can be referred to as reoxygenation and/or SmO₂ resaturation. Increases in the rate at which individuals can recover SmO₂ during intermittent rest periods throughout repeated bouts of exercise likely reflects a combination of improved restoration of metabolic factors (e.g., phosphocreatine) (Yoshida and Watari, 1993; Pilotto et al., 2022), faster reperfusion of oxygenated blood into the microcapillary networks within skeletal muscle, and larger O₂ delivery capacity. Thus SmO₂rate may change as intensity scales and the demands of skeletal muscle increase throughout a GXT, especially considering the documented disproportionate alterations in the metabolic milieu within skeletal muscle at circa-maximal exercise intensities (Brooks et al., 2022; Hargreaves et al., 1998; Yoshida and Watari, 1993). Collectively, available data is conflicting on the agreement between NIRS derived breakpoints and LT₁ and LT₂ (Sendra-Pérez et al., 2023), with some reports of very wide limits of agreement when compared to LT₂ specifically (Turnes et al., 2019). Additionally, less work has directly investigated changes in dynamic SmO₂ kinetics such as SmO₂rate and SmO₂resat.

Therefore, the purpose of this study was to investigate the association and agreement between SmO₂ breakpoints (SmO₂BP1 and SmO₂BP2) from the VL and LT₁ and LT₂ derived from discontinuous GXTs. In addition, longitudinal changes in the aforementioned physiological variables will be assessed across multiple time points during an entire academic year (August 2023 – May 2024). Further, secondary aims are to: 1) quantify the degree to which dynamic changes in SmO₂ during each GXT work-step (SmO₂rate) relate to dynamic changes in BLA kinetics, and 2) determine to what extent SmO₂ inter-step recovery kinetics change throughout GXTs. Collectively, the forthcoming analyses aim to provide additional insight on how VL SmO₂ kinetics change both acutely and longitudinally, as well as how SmO₂ kinetics relate to commonly measured BLA kinetics during GXT protocols in female rowing athletes.

Materials and methods

Experimental approach to the problem

A combination of cross-sectional and time-series research designs were employed in the present study. Data were collected at three pre-determined times in coordination with the University of Kansas' Women's Rowing Coaching Staff throughout the 2023–2024 academic year (September, November, and February), in alignment with the beginning of the Fall (Sept), end of the Fall (Nov), and just prior to the beginning of the main competitive season during the Spring academic term (Feb). A subset of

11 athletes were able to complete at least two repeat NIRS-equipped GXTs, with physiological data analyzed for longitudinal changes. The remaining 12 athletes performed a single GXT at one of the three aforementioned testing times. When comparing physiological variables from a single GXT across all 23 athletes, data from each athlete's first GXT of the 2023–2024 were used.

Subjects

Twenty-three National Collegiate Athletic Association (NCAA) Division I female rowing athletes performed the GXT protocol outlined in the present study as part of their routine longitudinal performance monitoring. According to McKay et al.'s proposed classification framework, these athletes are considered highly trained/national level (Tier 3) (McKay et al., 2022). All athletes were free of injury as cleared by the team's athletic trainers. Further, all athletes were screened for alcohol and tobacco use within the past 24-h and any upper respiratory tract infection symptoms within the last 2 weeks from the date of the GXT. This study was carried out in accordance to the 1964 Declaration of Helsinki, and the protocol was approved by the University of Kansas' institutional review board (STUDY#00150421).

Procedures

GXT protocol

The discontinuous 7x4-min rowing ergometer (Concept2 RowErg, Model D, Morrisville, Vermont, United States) step test employed was developed by the Australian Institute of Sport (Rice, 2019) to individualize training zone prescription based upon BLA and power outputs across seven steps of increasing intensity and (Rice, 2019). The workloads for steps one to six are based on each individual athlete's most recent personal best 2KErg, which was provided by members of the coaching staff from 2KErg testing conducted within the last 12 months (not their all time personal best), with step 7 being an all-out 4-min maximal effort. Throughout the 2023–2024 season, the GXT workloads at each step for each athlete were held constant, permitting changes in various physiological variables to be assessed longitudinally in response to the same protocol. The workload increases were consistent within each athlete but differed between athletes. For example, is an athlete's 2KErg was between 6:50–7:00 their workload would begin at 130 W and increase 25 W for steps one to six, whereas an athlete with a 2KErg of 7:40–7:50 would begin at 110 W and increase 15 W for steps 1–6. The 7x4-min GXT protocol provides a completely individualized approach for each athlete. Readers are referred to the most up-to-date protocol document for a step-by-step breakdown of this test (Rice, 2019). Athletes were instructed to avoid the consumption of any caffeine 12 h prior to all tests and to consume a pre-workout snack containing 30–60g carbohydrate 30–60min before all GXTs. Further, athletes were instructed not to consume any supplements on testing days. Prior to beginning, all athletes performed a 10-min warm-up on rowing ergometers at 10–15 W below their step 1 starting wattages. Baseline BLA samples were taken before and after the 10-min warm-up.

Blood lactate sampling and threshold determination

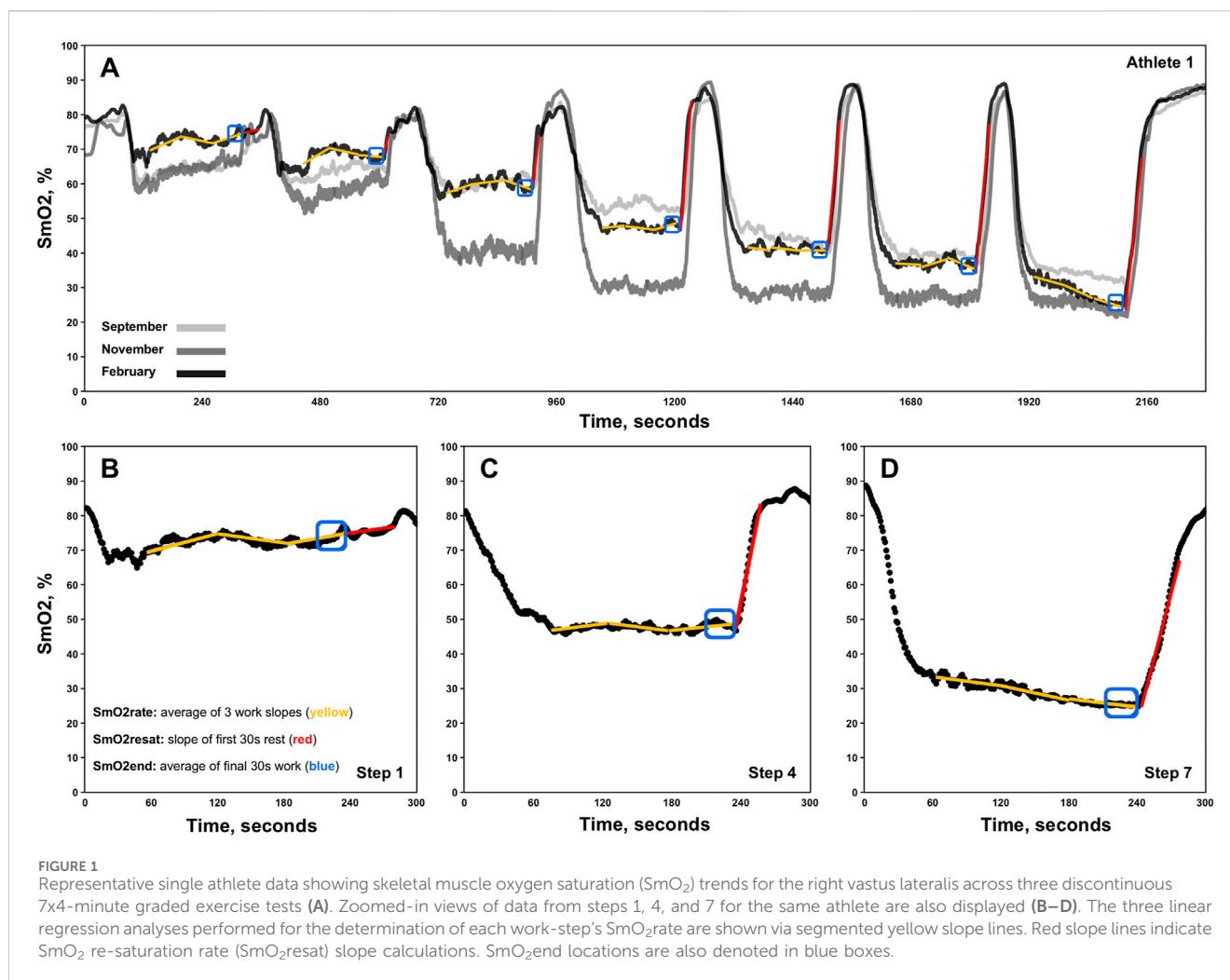
Finger-stick BLA measures were performed using a single-use disposable lancet and Lactate Pro two handheld analyzer (Arkray, Kyoto Japan), which has been shown to have strong intra-device reliability with intraclass correlation coefficients (ICC) = 0.99, with a coefficient of variation (CV) = 3.3% and 95% limits of agreement (LoA) between -1.0 and 1.0 mmol L⁻¹, making it ideal for testing in large team scenarios (Crotty et al., 2021). Prior to the beginning of the GXT, all athletes performed a 10-min warm-up on rowing ergometers at 10–15 W below their step 1 starting wattages. Baseline BLA samples were taken before and after the 10-min warm-up. All sampling was performed during the 1-min rest intervals of the discontinuous 7x4-min GXTs, with an additional sample taken 4 min after the maximal step to identify changes in BLA concentrations; the higher of the two readings (post-seventh step and +4 min) was used for each participant's peak BLA concentration and later used for determination of LT₁ and LT₂. Finger-stick samples were taken following cleansing of the site with an alcohol pad, with the first blood droplet wiped away (KimWipe, Kimberly-Clark Professional, Roswell GA) and the BLA test strip then touched to the second blood droplet. BLA thresholds were calculated using ADAPT software (Sport Alo, 1995) and were defined as follows (Bourdon, 2013): Lactate Threshold 1 (LT₁) is the intensity preceding a 0.4 mmol·L⁻¹ increase of BLA above baseline values and Lactate Threshold 2 (LT₂) is identified using the Modified DMax method, which draws a line from LT₁ to the finishing intensity and is the maximal distance of the line from the BLA curve (Bishop et al., 1998; Bourdon, 2013; Cheng et al., 1992).

NIRS data collection and preparation

Portable NIRS devices (MOXY Monitor, Fortiori Design LLC, Minnesota United States) were set to sample at a rate of 1 Hz (MOXY's "medium" setting) and affixed on the right VL at 1/3 the distance between the anterior superior iliac crest and the proximal, lateral-most patellar tip with CoverRoll stretch tape (Feldmann et al., 2019). The MOXY device uses an emitter with wavelengths at 690, 720, 760, and 800nm along with detectors placed 12.5 and 25mm from the emitter (McManus et al., 2018) providing real time data on the dynamic changes in skeletal muscle oxygenation saturation (SmO₂). SmO₂ is defined as the percentage of hemoglobin and myoglobin that is actively carrying oxygen within the capillaries and tissue of the muscle under investigation and is represented on a 0%–100% scale (Fortiori Design., 2016). NIRS data from all GXT trials were downloaded as Microsoft Excel files from the VO2 Master cloud software, and rowing ergometer power data was obtained from the rowing athlete management software system Ludum (Cambridge, UK).

NIRS inter-step recovery and work-rate parameters

SmO₂ resaturation rates (SmO₂resat) were calculated as the positive slope of the first 30s of SmO₂ data during each 1-min inter-step rest interval (Figure 1. Red lines) (Eserhaut et al., 2024). Exploratorily, mean SmO₂resat was calculated as a representative measure of local skeletal muscle recovery capacity across the entire GXT for each athlete with at minimum two sets of GXT NIRS data (n = 11). For SmO₂rate, the first 60s of each work step was ignored to



avoid the undue influence that the SmO_2 onset kinetics would have on subsequent calculations (Batterson et al., 2023). Three slopes were calculated for the remaining 60-s segments of each work step (e.g., 61–120, 121–180, 181–240s), with SmO_2 rate for each step representing the mean of these three work slopes (Figure 1. Yellow segmented lines). To determine both the degree of association and the shape of the relationships between SmO_2 rate and BLA, as well as SmO_2 rate and power, linear regression, second order polynomial, and inverse regression models were fit to the mean values for SmO_2 rate and BLA across all 7-steps for 23 sets of GXT data obtained, aligning with the first NIRS-equipped GXT performed by each athlete. Bayesian information criterion (BIC) and coefficients of determination (R^2) determine the best model fits (Chakrabarti and Ghosh, 2011). The mean SmO_2 from the final 30s of each work step (e.g., 210–240s) was calculated (SmO_2 end) for use in the forthcoming breakpoint analyses (Figure 1. Blue boxes).

NIRS breakpoint estimation

To determine SmO_2 breakpoints (SmO_2 BP1 and SmO_2 BP2) piecewise linear regression models were fit to the variables SmO_2 end and mean power (W), from the first GXT of the season performed by each individual athlete using the “segmented” package (version 2.1.0). Each piecewise model was specified to contain two

breakpoints ($npsi = 2$) prior to estimation. Briefly, the “segmented” package fits each model by minimizing the sum of squared residuals and testing for changes in linear slopes, providing estimated locations at which the slope of the relationship between y-axis variable (SmO_2 end) and x-axis variable (power) change to a statistically significant degree. Further details on the piecewise linear regression method used can be found in Muggeo, 2003) with a description of the “segmented” R-package (v2.1.0) available in Muggeo, 2008). Once breakpoint estimations were returned, researchers visually verified the breakpoint estimations via creating a scatter plot of SmO_2 end x Power overlaid with the segmented linear regression model.

Statistical analyses

All statistical analyses and data visualization were performed in R Studio (version 1.4.1106). A 1×7 repeated measures analysis of variance (RMANOVA) was used to determine if SmO_2 resat exhibited intensity dependent changes across the 7x4-min GXT protocol. Linear mixed-effects models were fit using the “lme4” package (version 1.1.34) to investigate mean differences (MD) in the variables mean SmO_2 resat, LT_1 , LT_2 , SmO_2 BP1, and

TABLE 1 Participant characteristics.

| Variable | Mean \pm SD |
|------------------------------------|-----------------|
| N | 23 |
| Age (years) ^a | 20.0 (18–22) |
| Height (cm) | 176.3 \pm 4.4 |
| Body Mass (kg) | 74.4 \pm 9.2 |
| On-Water Rowing Experience (years) | 3.0 \pm 2.2 |
| Indoor Rowing Experience (years) | 3.0 \pm 2.2 |
| 2,000-m Watts (W) ^a | 227 (205–305) |

^aNon-parametric variables, which are reported as median (range).

SmO₂BP2 across the fixed factor of time (e.g., September, November, February), using the individual athlete as a random factor [e.g., meanSmO₂resat \sim Time + (1 | ID)]. Within these models, restricted maximum likelihood (REML) estimates were used to account for missing repeated measures (Enders, 2006), with standard errors of the estimates (SEE) provided for the estimated marginal means of mean SmO₂resat, LT₁, LT₂, SmO₂BP1, and SmO₂BP2. Following significant univariate effects for time, *post hoc* Tukey HSD tests were performed.

Paired-samples t-tests were used to test for significant MD in LT₁ and SmO₂BP1, along with LT₂ and SmO₂BP2, with accompanying Cohen's *d* effect sizes. Effect size interpretation thresholds of small (0.2), medium (0.5), and large (0.8) were used (Cohen, 1988). Further, the two one-sided tests (TOST) procedure was used to test for statistical equivalence between LT₁ and SmO₂BP1, and LT₂ and SmO₂BP2 via the "TOSTER" package (version 0.8.3) (Lakens et al., 2018). Upper and lower equivalence bounds (Δ_U and Δ_L) were set to the *a priori* critical effect size for our study of $d = 0.6435$, given $n = 21$, our critical t-statistic of 2.086, and power (1- β err prob) of 0.8 (Lakens et al., 2018). Bland-Altman plots comparing LT₁ and SmO₂BP1, and LT₂ and SmO₂BP2 were created using the "BlandAltmanLeh" package (version 0.3.1), with linear regressions fit to the means and differences for LT₁ and SmO₂BP1, and LT₂ and SmO₂BP2, describing potential relationships between the direction of measurement biases and the magnitude of the thresholds. In addition to the Bland-Altman analyses, intraclass correlation coefficients were calculated using a single-measure, two-way mixed-effects model (ICC_{2,1}) to determine absolute agreement between the two physiological measurement methods using the "psych" package (version 2.4.6.26), with 95% confidence intervals (95% CI) also calculated (Shrout and Fleiss, 1979; Weir, 2005). Interpretations of poor (<0.5), moderate (0.5–0.75), good (0.75–0.9) and excellent (>0.9) were used (Koo and Li, 2016). Pearson product-moment correlations were also performed between LT₁ and SmO₂BP1, and LT₂ and SmO₂BP2 to determine the degree of association between the variables. Statistical interferences for all analyses were made using an *a priori* alpha level of $p \leq 0.05$.

Results

This cohort of NCAA Division I female rowers had 2KErg times ranging from 6:58.8 to 7:58.4 and had 3.0 \pm 2.2 years of on-water and

indoor rowing experience. Further descriptive statistics are reported in Table 1.

Acute SmO₂ resaturation rates

For SmO₂resat from the first NIRS equipped-GXT of the season ($n = 23$), a significant main effect for Time was present ($\eta^2_p = 0.71$, $p < 0.001$), with SmO₂resat clearly displaying marked intensity-dependent increases, as Tukey HSD *post hoc* comparisons between all steps yielded significant differences in SmO₂resat ($p < 0.01$), with the exception of step 5 – step 6 ($p = 0.064$), step 5 – step 7 ($p = 1.000$), and step 6 – step 7 ($p = 0.609$).

Longitudinal changes in mean SmO₂ resaturation rates

A significant univariate effect for mean SmO₂resat was present ($F = 4.35$, $p = 0.033$), indicative of changes across time. Tukey HSD *post hoc* comparisons yielded a significant reduction from Nov to Feb (MD = -0.21, SEE = 0.08, $df = 13.5$, $t = 2.69$, $p = 0.044$). Of note is the nearly significant elevation in mean SmO₂resat from Sept–Nov (MD = 0.21, SEE = 0.10, $df = 15.0$, $t = 2.19$, $p = 0.105$) that preceded this significant decline. Changes in both SmO₂resat during a single GXT and mean SmO₂resat across the season are shown in Figure 2.

SmO₂ work rates

Relationships between mean SmO₂rate, BLA, and power across the GXT protocol from 23 athletes are displayed in Figure 4. For SmO₂rate's relationship with BLA, linear regression ($R^2 = 0.48$, $p = 0.09$, $\sigma = 1.62$, BIC = 30.10) and second order polynomial ($R^2 = 0.73$, $p = 0.07$, $\sigma = 1.30$, BIC = 27.40) model fits were not statistically significant. However, plotting SmO₂rate against the inverse of BLA led to a strong statistically significant curvilinear fit ($R^2 = 0.92$, $p < 0.01$, $\sigma = 0.64$, BIC = 17.10). For the relationship between SmO₂rate and power, all models were significant. BIC and R-squared values indicated that a curvilinear second order polynomial best explains the relationship between SmO₂rate and power. Linear regression ($R^2 = 0.85$, $p < 0.01$, $\sigma = 0.86$, BIC = 21.20), second order polynomial ($R^2 = 0.99$, $p < 0.01$, $\sigma = 0.20$, BIC = 1.31), and inverse regression ($R^2 = 0.97$, $p < 0.01$, $\sigma = 0.41$, BIC = 10.80) all explained a significant proportion of the variance. The model fits are shown in Figure 3.

Differences and agreement between SmO₂ breakpoints and lactate thresholds

A significant difference was present between LT₁ and SmO₂BP1 ($t = -2.41$, MD = -8.14 [95% CI: -15.2 to -1.1], $d = 0.525$, $p = 0.026$), with poor-to-moderate agreement between the two measurement methods (ICC_{2,1} = 0.24 [95% CI: -0.13–0.58], $p = 0.10$). TOST equivalence testing also found LT₁ and SmO₂BP1 were not statistically equivalent ($t_{(40)} = 0.032$, $p = 0.487$, Δ_U and $\Delta_L = -8.33$ –8.33 W). Conversely, there was no significant

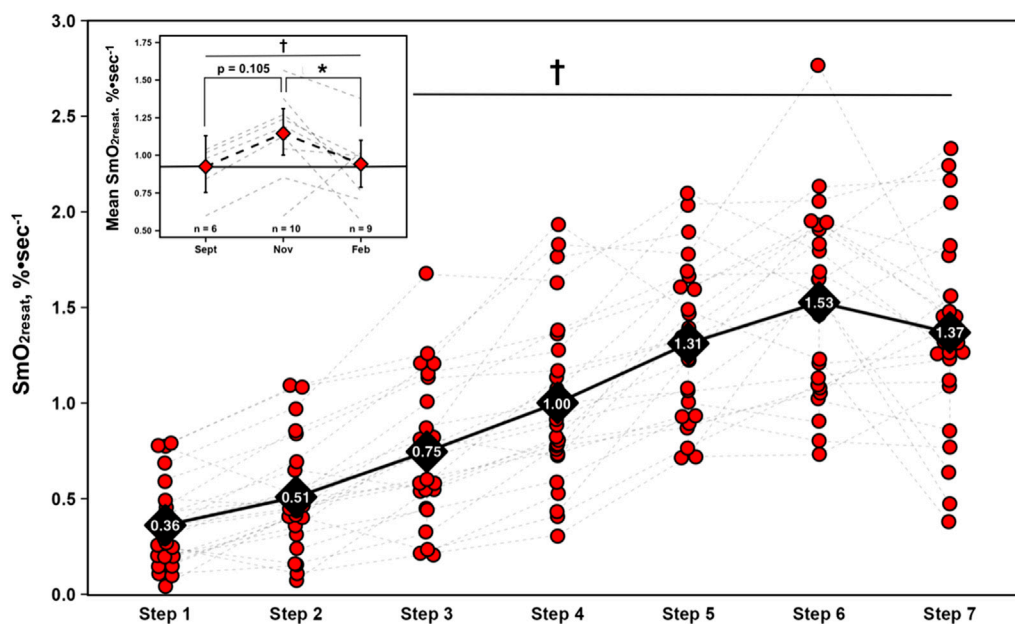


FIGURE 2 Skeletal muscle oxygen re-saturation rates (SmO_{2resat}) calculated as the slope of the first 30s of SmO_2 data during each 1-min inter-step rest interval from the first GXT completed with NIRS for $n = 23$ athletes. Individual data shown via red dots and gray dashed spaghetti plots. Black diamonds display mean values for each work-step, connected via solid black line. Top left figure inset presents longitudinal changes in mean SmO_{2resat} for a subset of athletes (total $n = 11$). Individual spaghetti plots are gray dashed lines, with estimated marginal means shown as red diamonds $\pm 95\%$ confidence intervals from the linear mixed-effects model, connected via black dashed line. Solid black line indicate Sept's means, treated as the baseline reference. † = main effect for Time ($p \leq 0.05$); * = significant difference ($p \leq 0.05$).

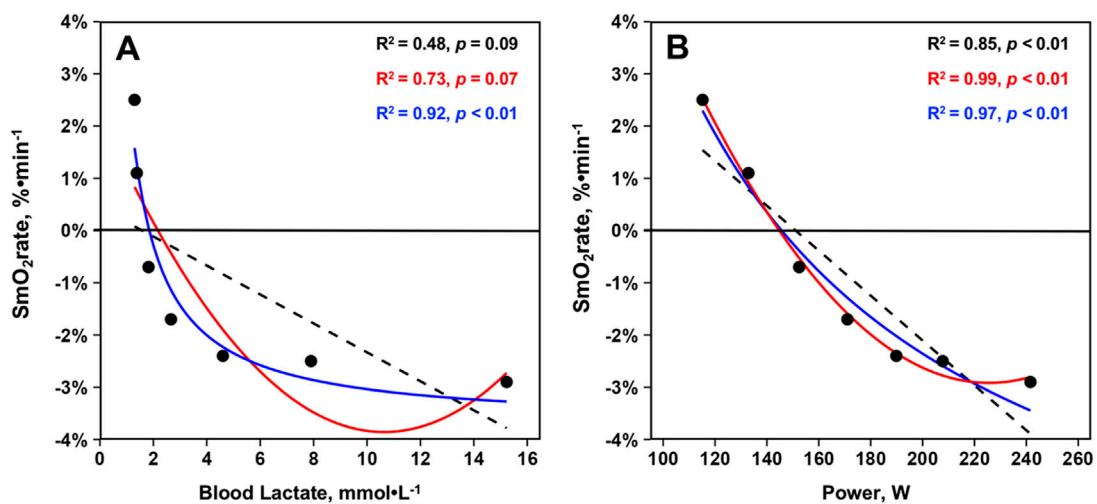


FIGURE 3 Mean skeletal muscle oxygen saturation rates (SmO_{2rate}) from the right vastus lateralis during the seven work-steps plotted against (A) mean blood lactates and (B) mean power outputs from the first GXT completed with NIRS for $n = 23$ athletes during the 2023–2024 season (23 total trials). Model fits displayed are simple linear regressions (black, dashed), second order polynomials (red, solid), and inverse regressions [formula: $y \sim 1/(1/x)$] (blue, solid). Variance explained by each model fit with statistical significance is displayed.

difference between the higher intensity thresholds LT_2 and SmO_{2BP2} ($t = -1.56$, $MD = -5.76$ [95% CI: -13.5 to 1.93], $d = 0.341$, $p = 0.134$), with these higher intensity thresholds possessing moderate-to-good levels of agreement ($ICC_{2,1} = 0.67$ [95% CI: 0.36 – 0.85], $p < 0.001$). However, TOST equivalence testing found LT_2 and SmO_{2BP2} were

not statistically equivalent ($t_{(40)} = 1.207$, $p = 0.117$, Δ_U and $\Delta_L = -13.77$ – 13.77 W). **Figure 4** shows the SmO_{2BP1} and SmO_{2BP2} and LT_1 and LT_2 for the athletes with the greatest agreement and least agreement between the two methods of physiological threshold determination. Additionally, individual

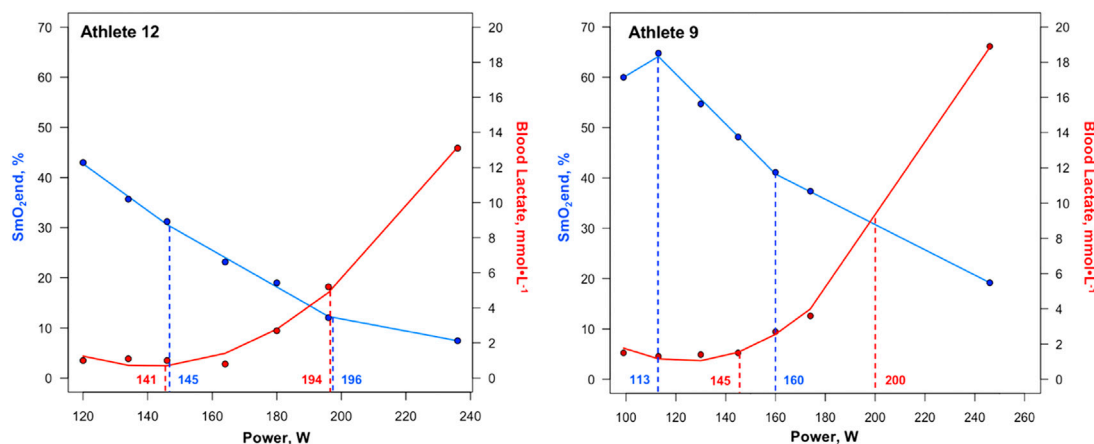


FIGURE 4
First and second SmO₂ breakpoints and lactate thresholds shown for athletes with the greatest agreement (Athlete 12) and least agreement (Athlete 9) between the two methods of physiological threshold determination. Solid blue lines represent segmented regression analyses, with dashed blue lines and accompanying power values demarcating SmO₂BP1 and SmO₂BP2. Solid red lines represent lactate curves generated using the ADAPT software, with dashed red lines and accompanying power values demarcating LT₁ and LT₂. SmO₂BP = skeletal muscle oxygen saturation breakpoint; LT = lactate threshold.

lactate threshold and SmO₂ breakpoint data for all athletes is displayed in [Table 2](#).

Bland-Altman plots displaying mean biases and 95% limits of agreement (95% LoA), along with the relationships between the two methods of physiological threshold determination, are displayed in [Figure 5](#).

Longitudinal changes in SmO₂ breakpoints and lactate thresholds

For the physiological thresholds determined, no significant univariate effects were present for any of the measured variables indicative of no statistically significant changes across the season. However, a trend toward a univariate effect for Time was present for SmO₂BP2 ($F = 2.715$, $p = 0.102$). Estimated marginal means and 95% confidence intervals from the mixed-effects models along with p-values from all non-significant Tukey HSD-adjusted pairwise comparisons are displayed in [Figure 6](#) for descriptive purposes.

Discussion

The purpose of this study was to investigate longitudinal changes in NIRS breakpoints and SmO₂ trends during GXT's performed across multiple time points during an entire academic year (August 2023– May 2024), along with determining the degree of agreement between NIRS and BLA methods of physiological intensity threshold identification. To the best of our knowledge, our study is the first to include longitudinal NIRS data on female rowers. The majority of NIRS rowing studies have focused on one to two trials to identify either HHb or TSI/SmO₂ breakpoints with most participants in these studies being male rowers ([Possamai et al., 2024](#); [Lanigan, 2022](#); [Turnes et al., 2019](#); [Klusiewicz et al., 2021](#)).

Further, SmO₂resat kinetics were also investigated for intensity-dependent changes and a possible high-intensity induced blunting effect. Exploratory, SmO₂resat values were averaged across GXTs for the athletes with longitudinal NIRS data and evaluated as a more generalized indicator of local muscle recovery capacity. Lastly, the dynamic intra-exercise balance between mQO₂ and mVO₂ was (SmO₂rate) was compared to mean BLA concentrations across this cohort of female rowers to provide insight into the shape of the relationship between SmO₂ kinetics during GXT work-steps and BLA concentrations per prior reports of linear and subtle curvilinear relationships in elite male soccer athletes ([Batterson et al., 2023](#); [Batterson et al., 2024](#)).

The principal findings with the greatest applied significance are that no difference was found between SmO₂BP2 and LT₂ (mean diff = $-5.76W$ [95% LoA = -38.52 to $22.25W$], $p = 0.134$), with moderate-to-good levels of agreement between the two ($ICC_{2,1} = 0.67$ [95% CI: 0.36 – 0.85], $p < 0.001$), and a significant positive relationship ($r = 0.69$, $p < 0.001$).

This was not the case for SmO₂BP1 and LT₁, with NIRS significantly underestimating LT₁ (mean diff = $-8.14W$ [95% LoA = -38.90 to $27.37W$], $p = 0.026$), with poor-to-moderate agreement ($ICC_{2,1} = 0.24$ [95% CI: -0.13 – 0.58], $p = 0.10$). Taken together, NIRS derived SmO₂ breakpoint determination does not appear to be a viable alternative for LT₁ determination, and despite the lack of a statistically significant difference in SmO₂BP2 and LT₂, notable inter-individual variance in agreement raises concerns about the use of NIRS as a standalone tool for training zone intensity prescriptions centered around LT₂. [Figure 4](#) highlights the range of differences between LT and SmO₂ breakpoints at the individual level, as from an applied perspective, if athlete 9 (panel B) utilized the SmO₂BP2 to anchor training session intensity, this would result in a markedly different training stimulus than their LT₂, resultantly different adaptations. Further, the piecewise linear regression modeling method used could not fit two sets of SmO₂ data from the 23 GXT trials analyzed for physiological breakpoints. This

TABLE 2 Individual SmO₂ breakpoints compared to lactate thresholds.

| Athlete | Power output, W | | Power output, W | |
|-----------|----------------------|--------------|----------------------|--------------|
| | SmO ₂ BP1 | LT1 | SmO ₂ BP2 | LT2 |
| 1 | 144 | 160 | 190 | 212 |
| 2 | 144 | 176 | 236 | 244 |
| 3 | 141 | 131 | 216 | 202 |
| 4 | 148 | 176 | 195 | 234 |
| 5 | 148 | 157 | 188 | 208 |
| 6 | 115 | 126 | 145 | 158 |
| 7 | 134 | 144 | 165 | 183 |
| 8 | 159 | 148 | 191 | 178 |
| 9 | 113 | 145 | 160 | 200 |
| 10 | 156 | 141 | 185 | 179 |
| 11 | 128 | 149 | 204 | 198 |
| 12 | 145 | 141 | 196 | 194 |
| 13 | - | - | - | - |
| 14 | 131 | 137 | 164 | 167 |
| 15 | 152 | 142 | 179 | 188 |
| 16 | 140 | 135 | 192 | 183 |
| 17 | 133 | 141 | 181 | 182 |
| 18 | 143 | 144 | 182 | 174 |
| 19 | 133 | 129 | 167 | 169 |
| 20 | - | - | - | - |
| 21 | 131 | 168 | 169 | 197 |
| 22 | 148 | 150 | 215 | 210 |
| 23 | 134 | 151 | 187 | 168 |
| Mean ± SD | 139.0 ± 11.9* | 147.2 ± 13.9 | 186.0 ± 21.0 | 191.8 ± 21.8 |

Individual threshold data presented are from the first test performed with NIRS by each athlete during the 2023–2024 season. “-” denotes NIRS data inadequate for piecewise linear regression analysis with two predetermined breakpoints. SmO₂BP = skeletal muscle oxygen saturation breakpoint; LT = lactate threshold; * = significant difference from LTs ($p \leq 0.05$).

suggests an 8.7% failure rate with the NIRS methods employed in this investigation when specifying two breakpoints are present prior to modeling.

The trend of NIRS underestimating the lactate thresholds measured could be in part due to limited oxygen availability within skeletal muscle preceding subsequent BLA accumulation. Thus, an inability to supply O₂ in quantities sufficient enough to match increasing O₂ demands locally within the skeletal muscle tissue (i.e., m $\dot{Q}O_2$) during higher intensity exercise limits the availability of O₂ within the vastus lateralis microcapillaries, evidenced by low absolute SmO₂ values (see step 7 in Figures 1, 4), which may serve as a rate-limiter in the mitochondrial oxidation of BLA and contribute to exponential rises in circulating BLA concentrations at higher exercise intensities. Thus, with limited O₂ availability within skeletal muscle microcapillaries may provide some physiological rationale as to why SmO₂BP2 trended towards underestimating LT₂. As for the

significant underestimating of LT₁ by SmO₂BP1, rather than a physiological reason, we posit that athletes expressing a positive SmO₂ curve during early GXT stages of the GXT where m $\dot{V}O_2$ is greater than m $\dot{Q}O_2$ during these lower exercise intensities biased some of the SmO₂BP1 estimations towards the left (see Figure 4, panel B, SmO₂BP1). Such positive SmO₂ curves have previously been reported during prolonged discontinuous bouts of mixed-intensity cycling where an increase in the absolute SmO₂ values occurs as exercise progresses (Yogev et al., 2023) indicating that a given individual is capable of supplying greater quantities of O₂ than is being demanded by the exercising musculature yielding increased available O₂ within muscle microcapillaries during exercise. This increase in SmO₂ has early on also been observed during treadmill GXTs where SmO₂BP1 was estimated to be in close proximity to this event in some athletes (Batterson et al., 2023). Thus, estimation of LT₁ using SmO₂ may be prone to inter-individual variances in their ability to deliver O₂ to exercising musculature during lower exercise

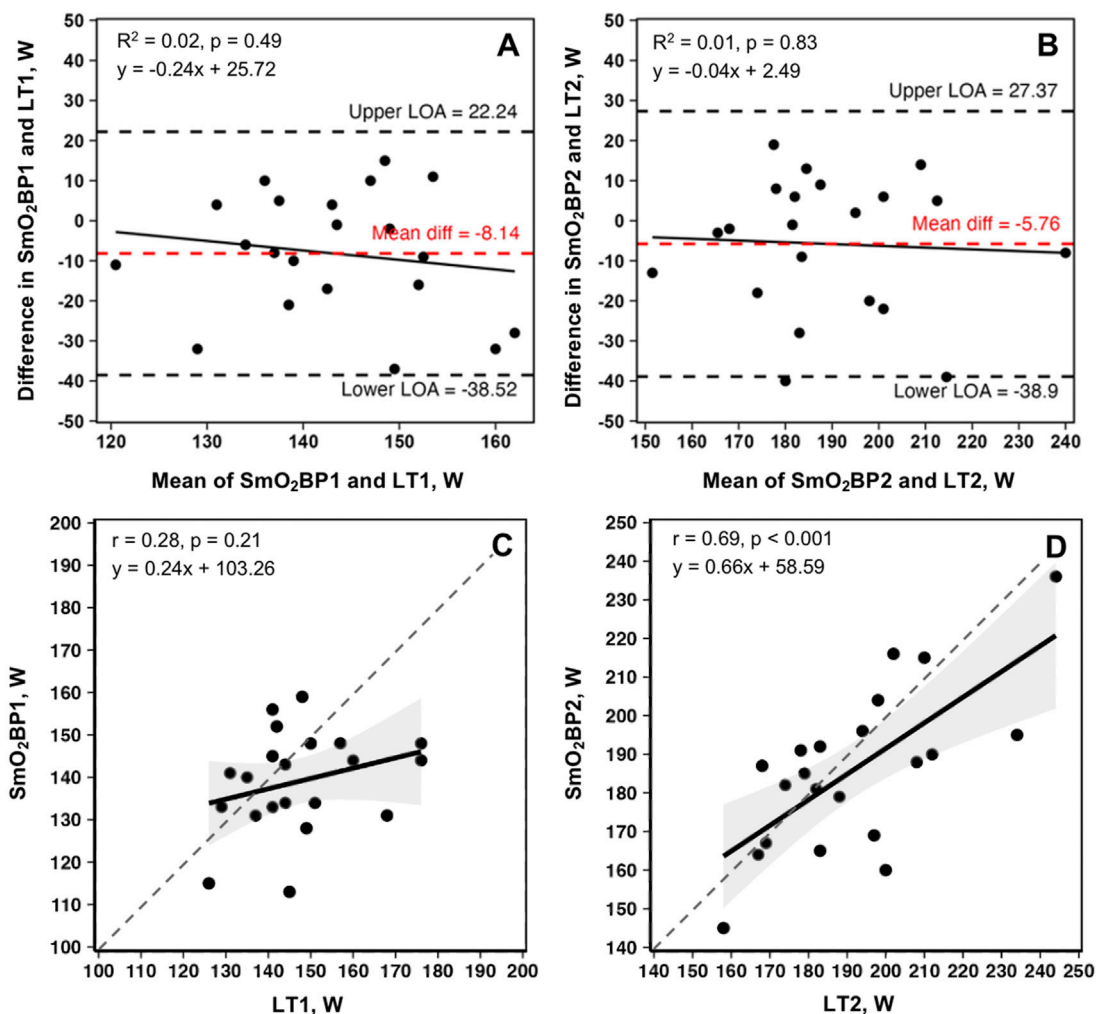


FIGURE 5
 Bland-Altman plots and linear regressions for SmO₂BP1 and LT₁ (A, C), and SmO₂BP2 and LT₂ (B, D) from the first NIRS equipped GXTs of the season for n = 21 athletes (21 total trials: one per athlete). Dashed red lines represent mean biases, with dashed black lines representing upper and lower 95% limits of agreement (LoA). Solid black lines show linear regressions, with gray dashed lines of agreement. Gray shaded areas are 95% confidence intervals. SmO₂BP = skeletal muscle oxygen saturation breakpoint; LT₁ = lactate threshold.

intensities. While our chosen 7x4-min GXT offers individualized starting intensities for each athlete (Rice, 2019), it may still be challenging to align step 1 with a wattage that yields a neutral to negative SmO₂rate throughout this 4-min piece with a high degree of consistency allowing practioners to avoid this positive SmO₂ curve at the start of testing. Further, when testing for statistical equivalence a very forgiving range of equivalence bounds (Δ_U and $\Delta_L = -13.77-13.77$ W) were used based upon our *a priori* critical effect size ($d = 0.6435$) calculated following methods of Lakens et al. (2018). Results showed a lack of equivalence between SmO₂BP1 and LT₁, and, despite a null mean difference between SmO₂BP2 and LT₂, no statistical equivalence was found for these higher intensity physiological threshold measures either, providing evidence that NIRS breakpoints, which are derived from local O₂ supply and demand kinetics within the skeletal muscle tissue of interest, are not inter-changeable with systemic BLA thresholds. This is not to say that SmO₂BP's and LT's, which both quantify notable metabolic events during exercise, are not related. Indeed, these significant

inflections in metabolic markers likely occur in a series of cascading events that take place during transitions across the exercise intensity spectrum and may influence one-another to some degree (Boone et al., 2016). However, despite SmO₂ and BLA kinetics being associated with one another physiologically, the two methods of monitoring human metabolism during exercise do not appear to be one and the same.

Of additional importance with respect to the logistics regarding data collection is that blood samples were taken during the 1-min rest period and are representative of BLA that has diffused into the capillaries at that moment in time compared to the NIRS breakpoints, which are the mean SmO₂ from the final 30s of each work step measured in real-time. The delay in time to collect the blood sample may be related to the differences between BLA and NIRS breakpoints as BLA levels have been shown to be dependent on the time to capture post-exercise, with longer post-exercise measurement times leading to lower BLA values (Vucetic et al., 2015). Furthermore, BLA threshold

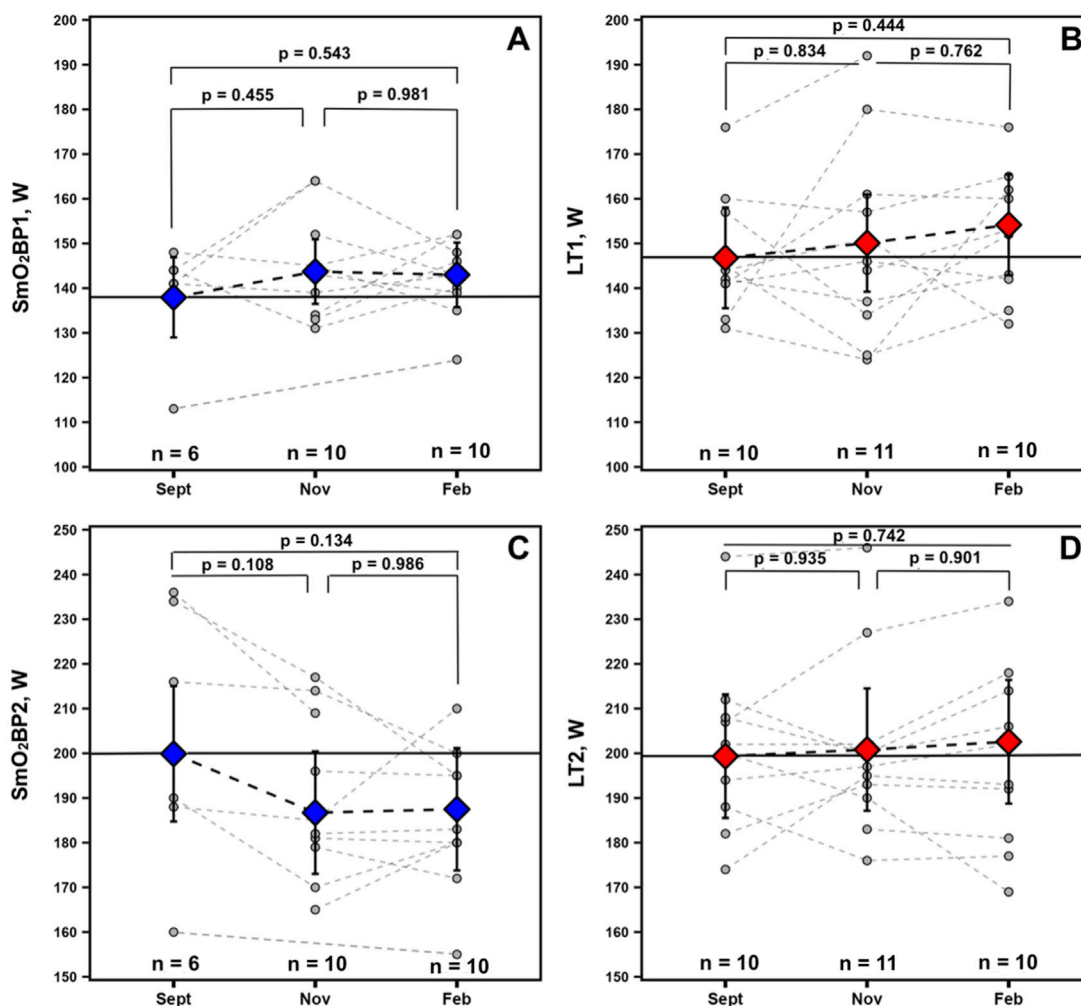


FIGURE 6 Data for athletes with at minimum 2 sets of GXT NIRS data are displayed. Individual spaghetti plots are gray dashed lines, with estimated marginal means \pm 95% confidence intervals from the linear mixed-effects models for SmO₂ breakpoints 1 and 2 (blue: A, C) and BLA thresholds 1 and 2 (red: B, D), connected via black dashed lines. Solid black lines indicate Sept's estimated marginal means, treated as the baseline reference.

determinations are highly dependent on the structure of the GXT protocol used and the method chosen to calculate LT₁ and LT₂ (Jannick et al., 2018). Importantly, NIRS thresholds likely also possess some degree of dependency on the structure and design of the GXT protocol chosen, and the breakpoint estimation method employed. For example, continuous GXTs yield an unbroken time-series of SmO₂ data (Feldmann et al., 2022) providing a greater quantity of data points to fit piecewise linear regression models which may produce SmO₂BP values that differ to some degree from those derived from discontinuous GXTs often required to conduct BLA testing during rowing ergometer trials.

The second finding of this investigation was that our cohort of NCAA Division I female rowers displayed a very curvilinear relationship between VL SmO₂rate and BLA. While this finding appears to agree with data from Batterson and colleagues, the shape of our regression model fits for the VL are dissimilar to the marked linear and subtle curvilinear relationships between SmO₂rate and BLA concentrations found during treadmill GXTs in elite male soccer athletes (Batterson et al., 2023; Batterson et al., 2024). This cohort of

female rowers showed marked declines in SmO₂rate during the early steps of the discontinuous 7x4-min GXT despite minimal changes in BLA, with the best model fit being very much curvilinear in nature (inverse regression: R² = 0.92, p < 0.01). This indicates SmO₂rate does not, on average, become increasingly negative above BLA levels of approximately 4–5 mmol·L⁻¹ (i.e., GXT Step #5), with SmO₂rate plateauing at a fairly stable -2.0%-3.0%·min⁻¹ throughout the remainder of the GXT in this cohort of female athletes (see Figure 3). Such a curvilinear relationship between SmO₂rate and BLA accumulation is akin to data from the long-head of the BF in other reports (Snyder and Parmenter, 2009; Brooks et al., 2022), a muscle that may reside under greater thicknesses of adipose tissue compared to the VL (Ishida et al., 1995). Further, sex differences in NIRS-derived values have been reported during vascular occlusion tests, with men desaturating and resaturating the VL at faster rates than women (Keller et al., 2023). Thus, the shape of the relationship between SmO₂rate and BLA accumulation throughout GXTs may differ as a function of sex, training status, exercise modality, GXT structure, or variance in adipose tissue thickness.

The final finding of this study was that SmO_2resat expresses intensity-dependent changes during graded exercise testing. With SmO_2 defined as the percentage of hemoglobin and myoglobin that is carrying oxygen to the capillaries (Fortiori Design, 2016), SmO_2resat represents the rate at which oxygen is replenished to the local muscle tissue (VL) during the 1-min rest intervals relative to the local skeletal muscle tissue's uptake of O_2 . After the all-out maximal efforts in step 7, SmO_2resat was no different from the sub-maximal workloads in step 6 ($p = 0.694$), demarcating a change in the statistically significant rate increases in SmO_2resat from steps 1–5. These findings are in agreement with recent findings by Arnold et al., 2024; Arnold et al., 2024). We posit this is potentially due to marked elevations in BLa, hydrogen ions, and overall disruption to the metabolic milieu within skeletal muscle at higher exercise intensities (Brooks et al., 2022; Hargreaves et al., 1998; Yoshida and Watari, 1993). High-intensity exercise also induces elevations in glycolysis leading to marked increases in acetyl-coenzyme A (acetyl-CoA), and, thereby, the formation of greater amounts of malonyl-coenzyme A (malonyl-CoA) (Brooks et al., 1999). Malonyl-CoA has been shown to downregulate the rate-limiting enzyme for mitochondrial β -oxidation of free-fatty acid derivatives, and as a result, oxygen is likely left available for use in transferring BLa into the mitochondrial matrix (Mcgarry et al., 1977; Saddik et al., 1993). We speculate that the blunting in SmO_2resat observed following the GXTs maximal seventh step effort may, in part, be related to the oxidative shuttling of BLa into the mitochondrial matrix for use as a readily available and abundant energy substrate during the immediate post-exercise recovery period. These same physiological factors may also explain, to some degree, the nonsignificant trend towards $\text{SmO}_2\text{BP2}$ underestimating LT_2 .

Furthermore, when averaged across the GXT and monitored longitudinally, mean SmO_2resat may be a variable worth monitoring for positive and negative adaptations to training programs and could serve as a sensitive proxy for short-to-moderate term fluctuations in training load. Athletes had nearly significant SmO_2resat elevations in Nov ($p = 0.105$) when their volumes of training were the highest with their low-intensity sessions completed below LT_1 ; these returned to near baseline values following winter break in Feb after a high-intensity training block with reduced volume. For the physiological thresholds LT_1 and $\text{SmO}_2\text{BP1}$, along with LT_2 , gradual increases were observed throughout the season. However, the magnitudes of these improvements were not statistically significant in this cohort. Interestingly, $\text{SmO}_2\text{BP2}$ appears to have declined throughout the season, the inverse of LT_2 . For mean SmO_2resat specifically, this may potentially reflect acute adaptation to the training program followed by some degree of detraining from winter break or a response to the high-intensity training block over the winter (see Figure 2). Increases in the rate at which individuals can recover SmO_2 during intermittent rest periods throughout repeated bouts of exercise likely reflects a combination of improved restoration of metabolic factors (e.g., phosphocreatine) (Yoshida and Watari, 1993; Pilotto et al., 2022), faster reperfusion of oxygenated blood into the microcapillary networks within skeletal muscle, and larger O_2 delivery capacity (Barstow, 2019). While mean SmO_2resat is an exploratory metric calculated by averaging the derived SmO_2resat metric from all seven post-step recovery windows, it may still provide some degree of signal into changes in the aforementioned physiological characteristics.

Limitations and future recommendations

First, skinfold thickness and/or adipose tissue measurements at the site of the NIRS device were not obtained. SmO_2 variables can be significantly skewed in individuals with skinfold thicknesses above 15mm (Feldmann et al., 2019). Thus, follow-up investigations should aim to monitor the variables presented in this investigation with a homogenous cohort of athletes with known skinfold thicknesses of sub-15mm, as inter-individual variances in skinfold thickness may introduce undesired variance into the data. Second, not all 23 athletes were able to perform two or more GXTs while equipped with a NIRS device due to various logistical challenges. Thus, future longitudinal studies should target larger sample sizes to provide increased clarity on the alterations in the investigated variables over time. Finally, while energy intake and exercise energy expenditure were not accounted for, the prevalence of relative energy deficiency in endurance sport athletes (REDs) (Mountjoy et al., 2023; Dasa et al., 2024), especially in females, may also impact SmO_2 kinetics. Finally, measures of SmO_2 recovery kinetics during discontinuous exercise (e.g., SmO_2resat and mean SmO_2resat) should be investigated in future studies to better elucidate their responsiveness to different training interventions, and potential utility as indicators of local physiological adaptations.

Conclusion

To the best of our knowledge, this is the first study monitoring SmO_2 breakpoints longitudinally across multiple GXTs in a cohort of highly trained female athletes. Wearable NIRS technology appears to be a non-invasive complimentary tool to BLa testing when worn during the chosen discontinuous 7x4-min GXT protocol, which is in agreement with prior research (Turnes et al., 2019). This is not the case for the lower intensity LT_1 , as NIRS significantly underestimated LT_1 in this population. Importantly, equivalence testing revealed that SmO_2 breakpoints and BLa thresholds are not statistically equivalent, providing evidence that the two are not interchangeable. Further analysis of SmO_2 kinetics show changes in SmO_2rate display clear curvilinear relationships with BLa concentrations throughout the rowing ergometer GXT, a divergence from the strong linear and subtle curvilinear relationships reported in prior work that used a treadmill GXT protocol with elite male soccer athletes (Batterson et al., 2023; Batterson et al., 2024). Lastly, while longitudinal trends in physiological thresholds are apparent, no statistically significant changes were found for either the LTs or SmO_2BPs monitored in this cohort throughout the season, which may be partially related to the change in training intensity and volume, size of the cohort monitored, nutritional factors such as energy availability, or other variables. Exploratorily, average GXT SmO_2resat (mean SmO_2resat) did display a significant reduction from Nov-Feb following winter break ($p = 0.04$), with a nearly significant improvement preceding it from Sept-Nov ($p = 0.105$) which is speculated to be reflective of short-to-moderate term changes in local metabolic O_2 exchange (i.e., $\dot{m}\text{QO}_2$ and $\dot{m}\dot{\text{V}}\text{O}_2$ balance) (Barstow, 2019) and microcapillary blood volume reperfusion rates (Keller et al., 2023) within the skeletal muscle tissue of interest, both of which may reflect an improved ability to sustain repeated bouts of exercise.

Data availability statement

The raw data supporting the conclusions of this article will be made available by the authors upon reasonable request, without undue reservation.

Ethics statement

The studies involving humans were approved by the University of Kansas' institutional review board. The studies were conducted in accordance with the local legislation and institutional requirements. The participants provided their written informed consent to participate in this study.

Author contributions

DE: Conceptualization, Data curation, Formal Analysis, Investigation, Methodology, Project administration, Visualization, Writing—original draft, Writing—review and editing. JD: Conceptualization, Data curation, Investigation, Methodology, Project administration, Writing—original draft, Writing—review and editing. JP: Data curation, Investigation, Methodology, Project administration, Writing—review and editing. KA: Methodology, Supervision, Writing—review and editing. AF: Methodology, Supervision, Writing—review and editing.

Funding

The author(s) declare that no financial support was received for the research, authorship, and/or publication of this article.

References

- Arnold, J. I., Yogev, A., Nelson, H., van Hooff, M., and Koehle, M. S. (2024), Muscle reoxygenation is slower after higher cycling intensity, and is faster and more reliable in locomotor than in accessory muscle sites after higher cycling intensity, and is faster and more reliable in locomotor than in accessory muscle sites. *Front. Physiol.* 15:1449384. doi:10.3389/fphys.2024.1449384
- Bangsbo, J., and Hellsten, Y. (1998). Muscle blood flow and oxygen uptake in recovery from exercise. *Acta Physiol. Scand.* 162 (3), 305–312. doi:10.1046/j.1365-201x.1998.0331e.x
- Barstow, T. J. (2019). Understanding near infrared spectroscopy and its application to skeletal muscle research. *J. Appl. Physiol.* 126(5): 1360–1376. doi:10.1152/jappphysiol.00166.2018
- Batterson, P. M., Kirby, B. S., and Feldmann, A. (2024). Response to: the remarkably tight relationship between blood lactate concentration and muscle oxygen saturation between blood lactate concentration and muscle oxygen saturation. *Eur. J. Appl. Physiol.* 124(1): 381–382. doi:10.1007/s00421-023-05361-7
- Batterson, P. M., Kirby, B. S., Hasselmann, G., and Feldmann, A. (2023). Muscle oxygen saturation rates coincide with lactate-based exercise thresholds coincide with lactate-based exercise thresholds. *Eur. J. Appl. Physiol.* 123(10): 2249–2258. doi:10.1007/s00421-023-05238-9
- Behnke, B. J., Ferreira, L. F., McDonough, P. J., Musch, T. I., and Poole, D. C. (2009). Recovery dynamics of skeletal muscle oxygen uptake during the exercise off-transient. *Respir. Physiol. Neurobiol.* 168(3): 254–260. doi:10.1016/j.resp.2009.07.013
- Bhambhani, Y., and Singh, M. (1985). Ventilatory thresholds during a graded exercise test. *Respiration* 47 (2), 120–128. doi:10.1159/000194758
- Bishop, D., Jenkins, D. G., and Mackinnon, L. T. (1998). The relationship between plasma lactate parameters, Wpeak and 1-h cycling performance in women Wpeak and 1-h cycling performance in women. *Med. Sci. Sports Exerc.* 30(8): 1270–1275. doi:10.1097/00005768-199808000-00014
- Bourdon, P. C. (2013). Blood lactate thresholds: concepts and applications. In: R. Tanner and C. J. Gore, editors. *Physiological tests for elite athletes*: Champaign, IL: Human Kinetics.
- Boone, J., Barstow, T. J., Celie, B., Prieur, F., and Bourgois, J. (2016). The interrelationship between muscle oxygenation, muscle activation, and pulmonary oxygen uptake to incremental ramp exercise: influence of aerobic fitness. *Appl. Physiol. Nutr. Metab.* 4(1): 55–62. doi:10.1139/apnm-2015-0261
- Brooks, G. A., Arevalo, J. A., Osmond, A. D., Leija, R. G., Curl, C. C., and Tover, A. P. (2022). Lactate in contemporary biology: a phoenix risen contemporary biology: a phoenix risen. *J. Physiol.* 600(5): 1229–1251. doi:10.1113/JP280955
- Brooks, G. A., Brown, M. A., Butz, C., Sicurello, J. P., and Dubouchaud, H. (1999). Cardiac and skeletal muscle mitochondria have a monocarboxylate transporter MCT1 mitochondria have a monocarboxylate transporter MCT1. *J. Appl. Physiol.* 87(5): 1713–1718. doi:10.1152/jappphysiol.1999.87.5.1713
- Chakrabarti, A., and Ghosh, J. K. (2011). AIC, BIC and recent advances in model selection. *Philos. Sci.* 7, 583–605. doi:10.1016/b978-0-444-51862-0.50018-6
- Cheng, B., Kuipers, H., Snyder, A., Keizer, H., Jeukendrup, A., and Hesselink, M. (1992). A new approach for the determination of ventilatory and lactate thresholds determination of ventilatory and lactate thresholds. *Int. J. Sports Med.* 13(7): 518–522. doi:10.1055/s-2007-1021309
- Cohen, J. (1988). *Statistical power analysis for the behavioral sciences* (2nd ed.). Hillsdale, NJ: Lawrence Erlbaum.
- Crotty, N. M., Boland, M., Mahony, N., Donne, B., and Fleming, N. (2021). Reliability and validity of the lactate Pro 2 analyzer lactate Pro 2 analyzer. *Meas. Phys. Educ. Exerc. Sci.* 25(3): 202–211. doi:10.1080/1091367X.2020.1865966
- Dasa, M. S., Friberg, O., Kristoffersen, M., Pettersen, G., Sagen, J. V., Torstveit, M. K., et al. (2024). Risk and prevalence of Relative Energy Deficiency in Sport (REDs) among

Acknowledgments

We would like to thank both the coaching staff and athletes of the University of Kansas' Women's Rowing team for their time, effort, and openness to collaboration. The authors would like to acknowledge funding support from the Joe and Clara Tsai Foundation. We are grateful for their commitment to furthering research on athletic performance.

Conflict of interest

JD owns and operates Science of Rowing, LLC a digital publication that publishes reviews of rowing research.

The authors declare that the research was conducted in the absence of any commercial or financial relationships that could be construed as a potential conflict of interest.

Generative AI statement

The author(s) declare that no Generative AI was used in the creation of this manuscript.

Publisher's note

All claims expressed in this article are solely those of the authors and do not necessarily represent those of their affiliated organizations, or those of the publisher, the editors and the reviewers. Any product that may be evaluated in this article, or claim that may be made by its manufacturer, is not guaranteed or endorsed by the publisher.

- professional female football players prevalence of Relative Energy Deficiency in Sport (REDs) among professional female football players. *Eur. J. Sport Sci.* 24(7):1032–1041. doi:10.1002/ejsc.12129
- Enders, C. K. (2006). A primer on the use of modern missing-data methods in psychosomatic medicine research. *Psychosom. Med.*, 68: 427–436. doi:10.1097/01.psy.0000221275.75056.d8
- Eserhaut, D. A., DeLeo, J. M., and Fry, A. C. (2024). Blood flow restricted resistance exercise in well-trained men: salivary biomarker responses and oxygen saturation kinetics men: salivary biomarker responses and oxygen saturation kinetics. *J. Strength Cond. Res.* 38(12): e716–e726. doi:10.1519/JSC.0000000000004913
- Faude, O., Kindermann, W., and Meyer, T. (2009). Lactate threshold concepts: how valid are they? *Sports Med.* 39, 469–490. doi:10.2165/00007256-200939060-00003
- Feldmann, A., Ammann, L., Gächter, F., Zibung, M., and Erlacher, D. (2022). Muscle oxygen saturation breakpoints reflect ventilatory thresholds in both cycling and running breakpoints reflect ventilatory thresholds in both cycling and running. *J. Hum. Kinet.* 83: 87–97. doi:10.2478/hukin-2022-0054
- Feldmann, A., Schmitz, R., and Erlacher, D. (2019). Near-infrared spectroscopy-derived muscle oxygen saturation on a 0% to 100% scale: reliability and validity of the Moxy Monitor saturation on a 0% to 100% scale: reliability and validity of the Moxy Monitor. *J. Biomed. Opt.* 24(11): 1–11. doi:10.1117/1.JBO.24.11.115001
- Fleming, N., Donne, B., and Mahony, N. (2014). A comparison of electromyography and stroke kinematics during ergometer and on-water rowing during ergometer and on-water rowing. *J. Sports Sci.* 32(12): 1127–1138. doi:10.1080/02640414.2014.886128
- Fortiori Design, L. (2016). *Muscle oxygen physiology course: Fortiori design*. LLC. Available at: <https://moxy-academy.teachable.com/>.
- Hagerman, F. C. (1984). Applied physiology of rowing. *Sports Med.* 1: 303–326. doi:10.2165/00007256198401040-00005
- Hargreaves, M., McKenna, M. J., Jenkins, D. G., Warmington, S. A., Li, J. L., Snow, R. J., et al. (1998). Muscle metabolites and performance during high-intensity intermittent exercise. *J. Appl. Physiol.* 84 (5), 1687–1691. doi:10.1152/jappl.1998.84.5.1687
- Homer, M. R. (2014). The physiological determinants of elite rowing performance: Implications for developing rowers (Liverpool John Moores university). Doctoral Thesis. Available at: <https://researchonline.ljmu.ac.uk/id/eprint/4338/>
- Iannetta, D., Qahtani, A., Maturana, F. M., and Murias, J. M. (2017). The near-infrared spectroscopy-derived deoxygenated haemoglobin breaking-point is a repeatable measure that demarcates exercise intensity domains. *J. Sci. Med. Sport.* 20(9): 873–877. doi:10.1016/j.jsams.2017.01.237
- Ishida, Y., Kanehisa, H., Carroll, J. F., Pollock, M. L., Graves, J. E., and Leggett, S. H. (1995). Body fat and muscle thickness distributions in untrained young females thickness distributions in untrained young females. *Med. Sci. Sport Exer.* 27(2): 270–274. doi:10.1249/00005768-199502000-00018
- Ingham, S., Whyte, G., Jones, K., and Nevill, A. (2002). Determinants of 2,000 m rowing ergometer performance in elite rowers. *Eur. J. Appl. Physiol.* 88(3): 243–246. doi:10.1007/s00421-002-0699-9
- Jamnack, N. A., Botella, J., Pyne, D. B., and Bishop, D. J. (2018). Manipulating graded exercise test variables affects the validity of the lactate threshold and [Formula: see text] affects the validity of the lactate threshold and VO₂peak. *PLoS One.* 13(7): e0199794. doi:10.1371/journal.pone.0199794
- Janshen, L., Mattes, K., and Tidow, G. (2009). Muscular coordination of the lower extremities of oarsmen during ergometer rowing during ergometer rowing. *J. Appl. Biomech.* 25(2): 156–164. doi:10.1123/jab.25.2.156
- Keir, D. A., Iannetta, D., Mattioni Maturana, F., Kowalchuk, J. M., and Murias, J. M. (2022). Identification of non-invasive exercise thresholds: methods, strategies, and an online app invasive exercise thresholds: methods, strategies, and an online app. *Sports Med.* 52(2): 237–255. doi:10.1007/s40279-021-01581-z
- Keller, J. L., Traylor, M. K., Gray, S. M., Hill, E. C., and Weir, J. P. (2023). Sex differences in NIRS-derived values of reactive hyperemia persist after experimentally controlling for the ischemic vasodilatory stimulus of reactive hyperemia persist after experimentally controlling for the ischemic vasodilatory stimulus. *J. Appl. Physiol.* 135(1): 3–14. doi:10.1152/jappphysiol.00174.2023
- Kindermann, W., Simon, G., and Keul, J. (1979). The significance of the aerobic-anaerobic transition for the determination of work load intensities during endurance training determination of workload intensities during endurance training. *Eur. J. Appl. Physiol. Occup. Physiol.* 42: 25–34. doi:10.1007/BF00421101
- Kirby, B. S., Clark, D. A., Bradley, E. M., and Wilkins, B. W. (2021). The balance of muscle oxygen supply and demand reveals critical metabolic rate and predicts time to exhaustion supply and demand reveals critical metabolic rate and predicts time to exhaustion. *J. Appl. Physiol.* 130(6):1915–1927. doi:10.1152/jappphysiol.00058.2021
- Kleshnev, V. (2016). *The biomechanics of rowing*. United Kingdom: The Crowood Press.
- Klusiewicz, A., Rębiś, K., Ozimek, M., and Czaplicki, A. (2021). The use of muscle near-infrared spectroscopy (NIRS) to assess the aerobic training loads of world-class rowers spectroscopy (NIRS) to assess the aerobic training loads of world-class rowers. *Biol. Sport.* 38(4): 713–719. doi:10.5114/biolsport.2021.103571
- Koo, T. K., and Li, M. Y. (2016). A guideline of selecting and reporting intraclass correlation coefficients for reliability research reliability research. *J. Chiropr. Med.* 15(2): 155–163. doi:10.1016/j.jcm.2016.02.012
- Lakens, D., Scheel, A. M., and Isager, P. M. (2018). Equivalence testing for psychological research: a tutorial. *Adv. Meth Pract. Psychol. Sci.* 1 (2), 259–269. doi:10.1177/2515245918770963
- Lanigan, B. (2022). Muscle oxygenation during graded exercise in trained rowers: Murdoch University. Masters Thesis. Available at: <https://researchportal.murdoch.edu.au/esploro/outputs/graduate/Muscle-oxygenation-during-graded-exercise-in/991005548666507891#details>
- Mader, A. (1976). Zur beurteilung der sportartspezifischen ausdauerleistungsfähigkeit. *Sportarzt Sportmed* 27, 80–88.
- Mader, A., Heck, H., and Hollman, W. (1978). “Evaluation of lactic acid anaerobic energy contribution by determination of post exercise lactic acid concentration of ear capillary blood in middle-distance runners and swimmers,” in *Exercise Physiology*. Editors F. Landry and W. Orban (Miami: Symposia Specialists), 187–200.
- Martin, S. A., and Tomescu, V. (2017). Energy systems efficiency influences the results of 2,000 m race simulation among elite rowers simulation among elite rowers. *Clujul Med.* 90(1): 60. 65. doi:10.15386/cjmed-675
- McGarry, J. D., Mannaerts, G. P., and Foster, D. W. (1977). A possible role for malonyl-CoA in the regulation of hepatic fatty acid oxidation and ketogenesis hepatic fatty acid oxidation and ketogenesis. *J. Clin. Invest.* 60(1): 265–270. doi:10.1172/JCI108764
- McKay, A. K. A., Stellingwerff, T., Smith, E. S., Martin, D. T., Mujika, I., Goosey-Tolfrey, V. L., et al. (2022). Defining training and performance caliber: a participant classification framework. *Int. J. Sports Physiol. Perform.* 17 (2), 317–331. doi:10.1123/ijspp.2021-0451
- McManus, C. J., Collison, J., and Cooper, C. E. (2018). Performance comparison of the MOXY and PortaMon near-infrared spectroscopy muscle oximeters at rest and during exercise PortaMon near-infrared spectroscopy muscle oximeters at rest and during exercise. *J. Biomed. Opt.* 23: 1–14. doi:10.1117/1.JBO.23.1.015007
- Mountjoy, M., Ackerman, K. E., Bailey, D. M., Burke, L. M., Constantini, N., Hackney, A. C., et al. (2023). 2023 international olympic committee’s (IOC) consensus statement on relative energy deficiency in sport (REDs). *Br. J. Sports Med.* 57 (17), 1073–1097. doi:10.1136/bjsports-2023-106994
- Muggeo, V. M. R. (2003). Estimating regression models with unknown break-points. *Stat. Med.* 22 (19), 3055–3071. doi:10.1002/sim.1545
- Muggeo, V. M. R. (2008). Segmented: an R package to fit regression models with broken-line relationships. *R. News* 8 (1), 20–25.
- Nugent, F. J., Flanagan, E. P., Wilson, F., and Warrington, G. D. (2020). Strength and conditioning for competitive rowers competitive rowers. *Strength Cond. J.* 42(3): 6–21. doi:10.1519/SSC.0000000000000531
- Pilotto, A. M., Adami, A., Mazzolari, R., Brocca, L., Crea, E., Zuccarelli, L., et al. (2022). Near-infrared spectroscopy estimation of combined skeletal muscle oxidative capacity and O₂ diffusion capacity in humans spectroscopy estimation of combined skeletal muscle oxidative capacity and O₂ diffusion capacity in humans. *J. Physiol.* 600: 4153–4168. doi:10.1113/jp283267
- Pollock, C. L., Jones, I. C., Jenkyn, T. R., Ivanova, T. D., and Garland, S. J. (2012). Changes in kinematics and trunk electromyography during a 2000 m race simulation in elite female rowers electromyography during a 2000m race simulation in elite female rowers. *Scand. J. Med. Sci. Sports.* 22(4): 478–487. doi:10.1111/j.1600-0838.2010.01249.x
- Possamai, L. T., Borszcz, F. K., de Aguiar, R. A., Lucas, R.Dd, and Turnes, T. (2024). Comparison of NIRS exercise intensity thresholds with maximal lactate steady state, critical power and rowing performance exercise intensity thresholds with maximal lactate steady state, critical power and rowing performance. *Biol. Sport.* 41(2): 123–130. doi:10.5114/biolsport.2024.129486
- R, P.-Q. J. I., Sanchez-Jimenez, J. L., Marzano-Felisatti, J. M., Encarnación-Martínez, A., and Salvador-Palmer, R. (2023). Reliability of threshold determination using portable muscle oxygenation monitors during exercise testing: a systematic review and meta-analysis. *Sci. Rep.* 13, 12649. doi:10.1038/s41598-023-39651-z
- Rice, A. J. (2019). 7 x 4 step test protocol. Available at: <https://rowingaustralia.com.au/wp-content/uploads/2019/09/RA-Pathways-Protocol-7-Step-Rowing-Protocol-2016-2020-Update-5-September-2019.pdf>.
- Rice, A. J. (2013). Rowers. In: R. Tanner and C. J. Gore, editors. *Physiological tests for elite*.
- Saddik, M., Gamble, J., Witters, L., and Lopaschuk, G. (1993). Acetyl-CoA carboxylase regulation of fatty acid oxidation in the heart acid oxidation in the heart. *J. Biol. Chem.* 268(34): 25836–25845. doi:10.1016/s0021-9258(19)74465-2
- Sendra-Pérez, C., Sanchez-Jimenez, J. L., Marzano-Felisatti, J. M., and Encarnación-Martínez, A. (2023). *Salvador-palmer*
- Shrout, P. E., and Fleiss, J. L. (1979). Intraclass correlations: uses in assessing rater reliability. *Psychol. Bull.* 86 (2), 420–428. doi:10.1037//0033-2909.86.2.420
- Snyder, A. C., and Parmenter, M. A. (2009). Using near-infrared spectroscopy to determine maximal steady state exercise intensity state exercise intensity. *J. Strength Cond. Res.* 23(6): 1833–1840. doi:10.1519/JSC.0b013e3181ad3362

- Soper, C., and Hume, P. A. (2004). Towards an ideal rowing technique for performance: the contributions from biomechanics. *Sports Med.* 34 (12), 825–848. doi:10.2165/00007256-200434120-00003
- Sport Alo (1995). "ADAPT. 6," in *Belconnen ACT: Australian Institute of sport.* 7 ed.
- Turnes, T., Penteado dos Santos, R., de Aguiar, R. A., Loch, T., Possamai, L. T., and Caputo, F. (2019). Association between deoxygenated hemoglobin breaking point, anaerobic threshold, and rowing performance. *Int. J. Sports Physiol. Perform.* 14 (8), 1103–1109. doi:10.1123/ijsp.2018-0675
- Turpin, N. A., Guével, A., Durand, S., and Hug, F. (2011). Effect of power output on muscle coordination during rowing during rowing. *Eur. J. Appl. Physiol.* 111(12): 3017–3029. doi:10.1007/s00421-011-1928-x
- Van Beekvelt, M. C. P., Shoemaker, J. K., Tschakovsky, M. E., Hopman, M. T. E., and Hughson, R. L. (2001). Blood flow and muscle oxygen uptake at the onset and end of moderate and heavy dynamic forearm exercise and muscle oxygen uptake at the onset and end of moderate and heavy dynamic forearm exercise. *Am. J. Physiology-Regulatory Integ Comp. Physiol.* 280(6): R1741–R1747. doi:10.1152/ajpregu.2001.280.6.R1741
- van der Zwaard, S., Weide, G., Levels, K., Eikelboom, M. R., Noordhof, D. A., Hofmijster, M. J., et al. (2018). Muscle morphology of the vastus lateralis is strongly related to ergometer performance, sprint capacity and endurance capacity in Olympic rowers. *J. Sports Sci.* 36(18): 2111–2120. doi:10.1080/02640414.2018.1439434
- Vucetic, V., Mozek, M., and Rakovac, M. (2015). Peak blood lactate parameters in athletes of different running events during low-intensity recovery after ramp-type protocol running events during low-intensity recovery after ramp-type protocol. *J. Strength Cond. Res.* 29(4): 1057–1063. doi:10.1519/JSC.0000000000000725
- Wasserman, K., and McIlroy, M. B. (1964). Detecting the threshold of anaerobic metabolism in cardiac patients during exercise. *Am. J. Cardiol.* 14(6): 844–852. doi:10.1016/0002-9149(64)90012-8
- Wasserman, K., Whipp, B. J., Koyle, S., and Beaver, W. L. (1973). Anaerobic threshold and respiratory gas exchange during exercise. *J. Appl. Physiol.* 35(2): 236–243. doi:10.1152/jappl.1973.35.2.236
- Weir, J. P. (2005). Quantifying test-retest reliability using the intraclass correlation coefficient and the SEM. *J. Strength Cond. Res.* 19(1): 231–240. doi:10.1519/15184.1
- Wilson, J.-M. J., Robertson, D. G. E., and Stothart, J. P. (1988). Analysis of lower limb muscle function in ergometer rowing ergometer rowing. *Int. J. Sport Biomech.* 4(4): 315–325. doi:10.1123/ijsb.4.4.315
- Yogev, A., Arnold, J., Nelson, H., Clarke, D. C., Guenette, J. A., Sporer, B. C., et al. (2023). The effect of severe intensity bouts on muscle oxygen saturation responses in trained cyclists intensity bouts on muscle oxygen saturation responses in trained cyclists. *Front. Sports Act. Living.* 5:1086227. doi:10.3389/fspor.2023.1086227
- Yoshida, T., and Watari, H. (1993). ³¹P-nuclear magnetic resonance spectroscopy study of the time course of energy metabolism during exercise and recovery course of energy metabolism during exercise and recovery. *Eur. J. Appl. Physiol. Occup. Physiol.* 66(6): 494–499. doi:10.1007/bf00634298